Electropolishing of steel in presence of some amines

A.M. Ahmed[a], M.A. Darweesh[b,*], Yassin Agour[c], M. Elzayett[a], W.A. Hammad[b]

[a] *Alxandria University, Faculty of Science, Alexandria, Egypt*
[b] *Tanta University, Faculty of Engineering, Egypt*
[c] *Damietta University, Faculty of Science, Egypt*

A B S T R A C T

Electropolishing of Steel in phosphoric acid is considered as corrosion rate of Steel and due to the economic importance of Steel, there are several researches deals with acceleration and inhibition of this process. This paper threw some light on the effect of adding some organic amines on the electropolishing of steel. Different concentration were used from 10^{-5} mol.L^{-1} to 10^{-2} mol.l^{-1} and different organic amines derivatives (methyl amine, dimethyl amine, diethyl amine, triethyl amine, diethanol amine and triethanol amine) were used. Electropolishing process of steel inhibited by different ratio. The results show that organic amines have strongest inhibiting effect ranging from 5% to 59.7% and the thermodynamic parameters as ΔS^*, ΔH^* and ΔG^* were studied. The values of ΔG_{ads} are given in negative values in all cases means that spontaneous adsorption of inhibitor on steel surface and strong interaction between the inhibitor molecules and metal surface. It lies in the range of (32–38) kJmol^{-1} for Flory - Huggins and (15–17) KJ mol^{-1} for kinetic isotherm. It's found that (ΔG_{ads}) values are more positive than -40 Kjmol^{-1} indicating that the inhibitors are physically adsorbed on the metal surface and the adsorption isotherm were given. The effect of amines compounds with nitrogen free, on the corrosion process is revealed by adsorption curves. The efficiency in inhibition decreases in the order: triethanol amine > diethanol amine > triethyl amine > diethyl amine > dimethyl amine > methyl amine.

1. Introduction

Electropolishing is widely employed in industry for micro finishing and debarring of different metallic components. A large number of electrolytic baths with different operating conditions are reported in the literature [1–4] but there is little information available on the mechanisms involved in Electropolishing in these systems. Most of the published work related to fundamental understanding of Electropolishing involved the study of Electropolishing of copper in phosphoric acid [5–12] although some work on steel, nickel, and chromium have also been reported [13–17]. In most of these studies electropolishing has been related to the existence of transport limited current plateau in the anodic polarization curve.

The corrosion of Steel and its alloy is of industrial concern that has received a considerable amount of attention. The corrosion of steel in acid media is important in the context of pickling, acid cleaning, etc. because of the general aggressiveness of acid solutions, the use of inhibitors to control the destructive attack of acid environment finds widespread application in many industries. A variety of organic compounds with functional groups containing heteroatom which can donate electron pairs are found to be useful as inhibitors in various media

[18].

Phosphoric acid H_3PO_4 is widely used in the protection of fertilizers and surface treatment of steel such as chemical and electrolytic polishing or etching, removal of oxide film, phosphating, passivating, and surface cleaning [19]. However, little work appears to have been done on the corrosion inhibition of steel in H_3PO_4. Hence,

The aim of this work is to examine the corrosion behavior of steel in H_3PO_4 in the presence of low price, low toxicity and easy production surfactants.

The aim of this study is the analysis of the effect of some amine derivatives for the inhibition of steel corrosion in 8 M H_3PO_4 at different conditions. The rate of steel corrosion is determined by measuring the anodic limiting current.

2. Experimental

2.1. Materials

Analar BHD chemical were used: (i) H_3PO_4 (98% w/w) (ii) methyl amine(iii) dimethyl amine (iv)diethyl amine(v) triethyl amine(vi) diethanol amine and (vii) triethanol amine double distilled water used to

---

Nomenclature

(a)	Methyl amine
A	Frequency factor
(b)	Dimethyl amine
(c)	Diethyl amine
C	Inhibitor concentration in the bulk solution
CI	Concentration and Θ is surface coverage
D	Diffusion coefficient of $Fe+2$ ($cm^2\ s^{-1}$)
(d)	Triethyl amine,
(e)	Diethanol amine
E_a	Activation energy ($kJ.mol-1$)
(f)	Triethanol amine
$f(\Theta,x)$	Configuration factor
ΔG	Net free energy change ($kJ.mol^{-1}$),
(ΔG_{ads})	Free energy of adsorption at different concentrations of the natural products
h	Plank's constant,
Δ	H change in enthalpy ($kJ.mol^{-1}$),
I	Limiting current

(I_{blank})	Limiting current in absence of amines
($I_{organic}$)	Limiting current in the presence of organic amines
K	Equilibrium constant of adsorption process,
k	Boltzmann's constant, e = 2.7183,
K	Binding constant of adsorption $K = k'^{1/y}$
k'	Binding constant
R	Gas constant (the universal gas constant)($8.314\ kJ.mol-1$),
ΔS	Change in entropy ($J.mol^{-1}.\ K^{-1}$)
T	Absolute temperature (K).
X	Size ratio is the number of water molecules displaced by one molecule of organic inhibitor
y	Number of inhibitor molecules occupy one active site.
1/y	Number of the active surface sites occupied by one molecule of the inhibitor
η	Viscosity of the solution ($g.cm^{-1}\ s^{-1}$)
(β)	Isokinetic temperature
Δ	Difference between any two reactions in series
(Θ)	Degree of surface coverage (the surface coverage) at given concentration

prepare the electrolyte.

2.2. Apparatus and procedure

Fig. 1. Represents the components of the cell and the electrical circuit that has been used in this work. The cell is made of a rectangular plastic container with dimensions ($5.1 \times 5.0 \times 10.0$ cm) with electrodes fitting the whole section. Two electrodes, each as rectangular steel plate of 10 cm height and 5 cm width, are located 5.1 cm apart. A porous poly vinyl chloride diagram is used to prevent the effect of H_2 bubble.

The electrical circuit used in this work consists of 6 V D.C. power supply of 6 V with a voltage regulator and multi-range ammeter is connected in series with cell. Potential differences are obtained by increasing the cell current stepwise and measuring the steady state anode potential against a reference electrode consist of a Steel wire immersed in a cup of Luggin probe filling with solution at concentration similar to that in the cell, the tip of Luggin probe is placed 0.5–1 mm tube from the anode surface.

The Potential difference between the anode and the reference electrode is measured by high impedance potentiometer. Ortho-phosphoric acid concentration is prepared from Analar ortho-phosphoric acid and distilled water. The anode height is 2 cm. before each run the block part of the anode is insulated with poly-styrene lacquers and the active surface of the anode is polished with fine emery paper, degreased with trichloroethylene, Washed with alcohols and finally rinsed in distilled water. Electrode treatment is similar to that used by Wilke [20]. The rate of Steel corrosion under different conditions is determined by measuring the limiting Current at 25 °C. Six different concentration of organic amines with 8 M H_3PO_4.

3. Results and discussions

3.1. Leveling process

The principle in electro-polishing is called leveling [21–23]. It can be explained by mass transfer mechanism [21]. A cell with a diaphragm has been used in this study. The use of this cell eliminates the effect of the evolved hydrogen gas at the cathode from affecting the rate of mass transfer at the anode, that is, natural of mass by convection. A cell

without diaphragm is used to study the effect of hydrogen gas evolved at the cathode on the rate of mass transfer at the anode, i.e., forced convection. The study of leveling is based on the classical current voltage curves of electro-polishing (as shown in Fig. 2). A typical polarogram is obtained in this study for triethanol amine in both cases of divided and undivided cell. The curve is divided into three stages: A) The first stage, the current density(c.d) is proportional to the voltage. B) The second stage of the curve, the metal undergoes electro-polishing. In the first stage, etching takes place as well as in last part, some localized pitting occurs [22].

3.2. Effect of Amine concentration on the limiting current

The observed limiting current, which represents the rate of Steel metal anodic corrosion in phosphoric acid at different temperature, are found that, the limiting current decrease with increasing the concentration of organic amines. Fig. 3 shows the dependence of limiting current on the bulk concentration in absence and in presence of organic amines. It has been found that, the limiting current deceases with increasing the concentration of organic amines. From the practical point of view, we can recommend on the basis of results that, it may use in this range of concentration to inhibit the corrosion of steel in 8 M H_3PO_4 acid in all types of amines to be used in this work

When the limiting current in absence of amines (I_{blank}), and in the presence of organic amines ($I_{organic}$), the percentage of inhibition can be calculated from the following equation
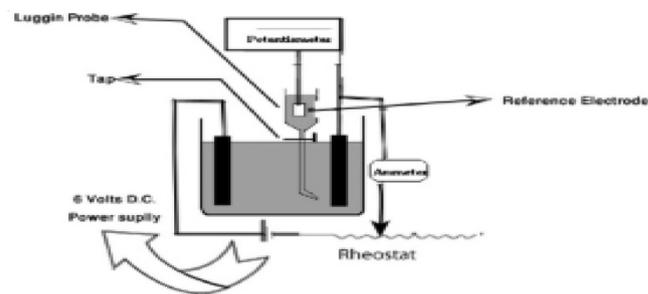
Fig. 1. The electrolytic cell and the electrical circuit.
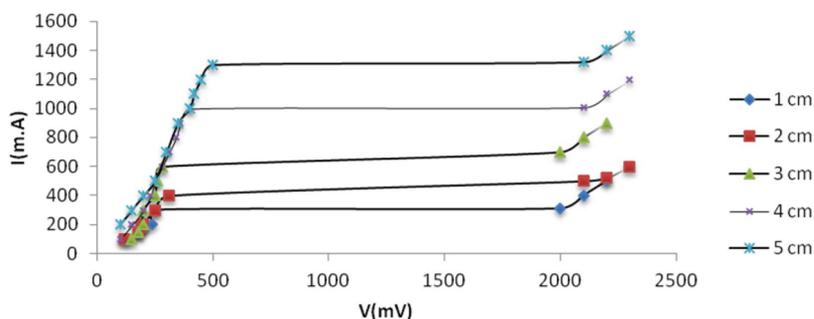
Fig. 2. The relation between the current and potential at different electrode height, in 8 M H$_3$PO$_4$, and the temp is 25 °C.
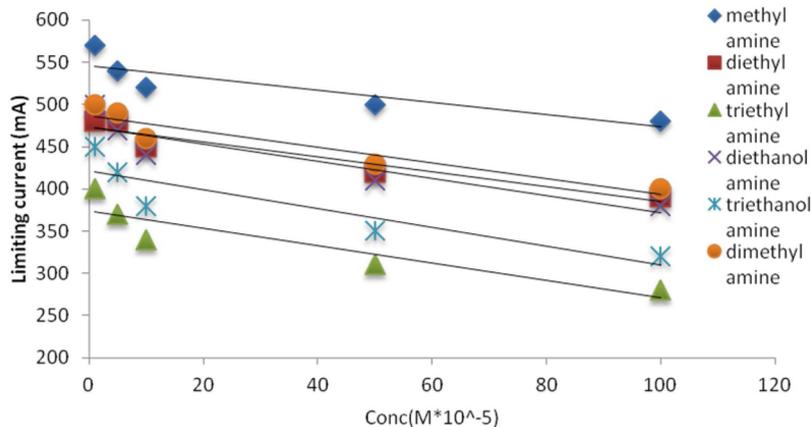
Fig. 3. The relation between limiting current and amines concentration at 25 °C.
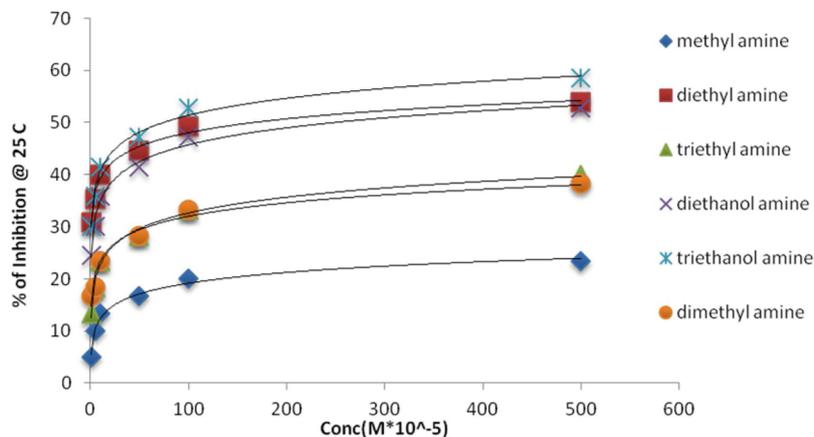
Fig. 4. Relation between concentration and % of inhibition at 25 °C.

$$\%\text{inhibition} = \frac{I_{blank} - I_{organic}}{I_{blank}} \times 100 \qquad (2)$$

Fig. 4 and Table 1 show that, the percent inhibition caused by organic amines range from 5% to 59.9% depending on amine type and its concentration.

With increasing the concentration of amines the limiting current decreases and this agree with the finding of other authors whom worked within the same range of concentration using other anode geometries [24,25] The decreasing in the limiting current with increasing with amine concentration can be explained with the following reasons

1 The solubility of dissolved Ferrous phosphate in ortho phosphoric acid, which is responsible for the limiting current, decreases with increasing amine concentration
2 Increasing the viscosity of the solution with increasing amine concentration, with consequence decrease in the diffusivity of Fe^{+2}

Table 1
The values of limiting current (mA) at different temperatures (25 °C–40 °C) for all compounds used in case of divided cell.

Conc. M×10⁵	Methyl amine				Dimethyl amine			
	25 °C	30 °C	35 °C	40 °C	25 °C	30 °C	35 °C	40 °C
0.0	600	650	690	720	600	650	690	720
1	570	590	610	630	500	550	580	620
5	540	570	590	610	490	520	550	590
10	520	540	560	580	460	490	520	560
50	500	520	540	560	430	460	490	530
100	480	500	520	540	400	430	460	500
500	460	480	500	520	370	400	430	460

Conc. M×10⁵	Diethyl amine				Triethyl mine			
	25 °C	30 °C	35 °C	40 °C	25 °C	30 °C	35 °C	40 °C
0.0	650	700	760	820	600	650	690	720
1	450	500	500	600	520	560	590	620
5	420	470	520	570	490	530	560	590
10	390	440	490	540	460	500	530	560
50	360	410	460	510	430	470	500	530
100	330300	380	430	480	400	430	470	500
500		350	400	460	360	410	440	470

Conc. M×10⁵	Diethanol amine				Triethanol amine			
	25 °C	30 °C	35 °C	40 °C	25 °C	30 °C	35 °C	40 °C
0.0	530	560	590	620	530	560	590	620
1	400	430	460	490	370	400	430	400
5	370	400	430	460	340	370	400	370
10	340	370	400	430	310	340	370	340
50	310	340	370	400	280	300	340	310
100	280	310	350	370	250	270	310	280
500	250	280	310	340	220	240	250	250

Percent of inhibition for organic compounds at different concentrations for divided cell.

Table 2
The relation between percentage inhibition and concentration of all compounds at 25 °C, divided cell.

C x 10⁵ mol.l⁻¹	% Inhibition					
	Methyl amine	Dimethyl amine	Diethyl amine	Triethyl amine	Diethanol amine	Triethanol amine
1.0	5	16.6	30.8	13.3	24.5	30.2
5	10	18.3	35.4	18.3	30.1	35.8
10	13.3	23.3	40	23.3	35.8	41.5
50	16.6	28.3	44.6	28.3	41.5	47.2
100	20	33.3	49.2	33.3	47.2	52.8
500	23.3	38.3	53.8	40	52.8	58.5

Table 3
The relation between percentage inhibition and concentration of all compounds at 30 °C for divided cell.

C x 10⁵ mol.l⁻¹	% Inhibition					
	Methyl amine	Dimethyl amine	Diethyl amine	Triethyl amine	Diethanol amine	Triethanol amine
1.0	9.2	15.3	28.6	13.8	23.2	28.6
5	12.3	20	32.9	18.5	28.6	33.9
10	16.9	24.6	37.1	23.1	33.9	39.3
50	20	29.2	41.4	27.7	39.2	46.2
100	23.1	33.8	45.7	33.8	44.6	51.8
500	26.2	38.4	50	36.9	50	57.1

Table 4
The relation between percentage inhibition and concentration of all compounds at 35 °C, for divided cell.

C x 10⁵ mol.l⁻¹	% Inhibition					
	Methyl amine	Dimethyl amine	Diethyl amine	Triethyl amine	Diethanol amine	Triethanol amine
1.0	11.6	15.9	34.2	14.5	22.0	27.1
5	14.5	20.2	31.6	18.8	27.1	32.2
10	18.8	24.6	35.5	23.2	32.2	37.3
50	21.7	28.9	39.5	27.5	37.3	42.3
100	24.6	33.3	43.4	31.9	40.7	47.5
500	27.5	37.6	47.4	36.2	47.5	57.6

Table 5
The relation between percentage inhibition and concentration of all compounds at 40 °C, for divided cell.

C x 10⁵ mol.l⁻¹	% Inhibition					
	Methyl amine	Dimethyl amine	Diethyl amine	Triethyl amine	Diethanol amine	Triethanol amine
1.0	12.5	13.8	26.8	13.9	21	35.5
5	15.3	18	30.5	18.1	25.8	40.3
10	19.4	22.2	34.1	22.2	30.6	45.2
50	22.2	26.3	37.8	26.4	35.5	50
100	25	30.5	41.5	30.6	40.3	54.8
500	27.8	36.1	43.9	34.7	45.2	59.7

according to Stokes-Einstein equation [26].

$$\eta\, D\, /T = constant \qquad (3)$$

Where: η is the Viscosity of the solution (g.cm⁻¹ s⁻¹).

D is the diffusion coefficient of Fe^{+2} (cm 2 s⁻¹), and T is the absolute temperature (K).

Also the increase in solution viscosity with increasing in phosphoric acid concentration results in an increase in the diffusion layer thickness which represent the resistance to the rate of mass transfer of Fe^{+2} from anode surface to the bulk solution (Tables 2–5).

3.3. Adsorption isotherms

It is generally agreed that the adsorption isotherm of the inhibitor at the metal interface is the first main role of the mechanism of inhibitors action in aggressive acid media. Four types of adsorption may take place in the inhibition phenomena involving organic molecules at the metal-solution interface namely:

a) Electrostatic attraction between charged molecules and metal.
b) Interaction of lone pairs of electron in the molecules with the metal.
c) Interaction of electrons with the metal.
d) A combination of the above [27].

Chemisorptions involves sharing or charge transfer from the inhibitor molecule to the metal surface in order to form a coordinate bond, in fact, electron transfer is typical in transition metals having vacant low energy electron orbital.

Concerning inhibitors, electron transfer can be expected with compounds having relatively loosely bound electrons. This situation may arise because of the presence (in adsorbed inhibitor) of multiple bonds or aromatic rings of a Π character [28–35].

The inhibition efficiency of homologous series of organic substances, differ only in the heteroatom, is usually in the following sequence:

P > Se > S > N > O

Table 6
The values of K,X and 1/Y of amines according to Longmuir, Flory – Huggins, and Kinetic Adsorption Isotherm.

Compound	Flory – Huggins		Longmuir	Kinetic Adsorption Isotherm			
	X	K	K	K'	Y	1/Y	K
Methyl amine	21.54	9819	153.84	2.86	0.27	3.64	10.62
Dimethyl amine	15.84	10001	11.57	1.83	0.26	3.91	7.05
Diethyl amine	13.30	239085	3.77	2.78	0.16	6.26	17.42
Triethyl amine	13.51	5359	38.4	2.49	0.24	4.21	10.36
diethanol amine	12.10	37087	8.16	3.36	0.20	4.89	16.81
Triethanol amine	10.18	86843	5.59	1.04	0.05	20.83	20.83

Table 7
The calculated values of free energy of adsorption, ΔG_{ads}, (K.J. mol^{-1}) of organic amines.

Compound	Longmuir -ΔG_{ads} KJ mol^{-1}	Flory – Huggins -ΔG_{ads} KJ mol^{-1}	Kinetic Adsorption Isotherm -ΔG_{ads} KJ mol^{-1}
Methyl amine	22.4	32.15	15.75
Dimethyl amine	16.02	32.97	14.80
Diethyl amine	13.24	40.66	17.04
Triethyl amine	19.00	30.90	15.75
diethanol amine	15.16	36.04	16.95
Triethanol amine	14.22	38.15	17.50

The electrochemical processes on the metal surface are likely to be closely to the adsorption of the inhibitor which is known to depend on the structure of the inhibitor [36].

The Adsorption of the inhibitor molecules from aqueous solutions can be regarded as substitution adsorption process between the organic compound in the aqueous phase, (org.$_{(aq.)}$) and the water molecules at the electrode surface, ($H_2O_{(s)}$).

$$Org_{(aq)} + xH_2O_{(s)} = Org_{(s)} + x (H_2O) \tag{4}$$
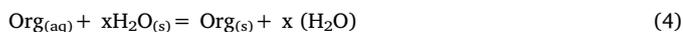
Where X (the size ratio) is the number of water molecules displaced by one molecule of organic inhibitor.

Adsorption isotherms are very important in determining the mechanism of organo-electrochemical reactions. The most frequently used isotherms are those of Langmuir, Frumkin, Parsons, Temkin, FIory-Huggins, and Bockris-Swinkels [37]. These entire isotherms are of the general form:

$$f(\Theta,x) \exp^{[-a\Theta]} = KC \tag{5}$$

where $f(\Theta,x)$ is the configuration factor depends essentially on the physical model and assumption underlying the derivation of the isotherm. The mechanism of inhibition is generally believed to be due to the formation and maintenance of a protective film on the metal surface [38].

$$\Theta = I-(I_L-I) \tag{6}$$

The degree of surface coverage (Θ)

Inhibitors adsorption characteristics can be estimated by using the Langmuir isotherm given by: [35]

$$KC = (\Theta/1)-\Theta \tag{7}$$

Where K is the equilibrium constant of adsorption process, C is the concentration and Θ is surface coverage.

Inhibitors adsorption characteristics can be done using Langmuir isotherm

$$C/\Theta = C + 1/k \tag{8}$$

where K is the equilibrium constant of adsorption process, C is the inhibitor concentration in the bulk solution and Θ is the surface coverage. By plotting C/Θ & C, it is found that Langmuir isotherm doesn't verified by those results.

This explains:

i   There is no interaction between adsorbed molecules
ii The energy of adsorption is independent on the surface coverage
iii The solid surface contains a fixed number of adsorption sites and each hole adsorbed species

Fig.5 and Tables 6 and 7 show the Flory-Huggins adsorption isotherm for copper electrode in H_3PO_4 solution, plotted as log Θ /C against log (1- Θ) at different temperatures. Straight lines are obtained with a slope X and intercept log x K. The experimental data fit the Flory-Huggins adsorption isotherm which is represented by:

$$\log \Theta/C = \log x k + x \log (l-\Theta) \tag{9}$$

where x is the number of water molecules replaced by one molecule of the inhibitor. The adsorption of inhibitors at metal-solution interface may be due to the formation of electrostatic or covalent bonding between the adsorbents and the metal surface. [39]

The kinetic thermodynamic isotherm may be written in the form [40] (Fig. 5)

$$\log(\Theta/1)-\Theta = \log K' + y \log C \tag{10}$$

Where y is the number of inhibitor molecules occupy one active site. The binding constant of adsorption $K = k'^{1/y}$, where 1/y is the number of the active surface sites occupied by one molecule of the inhibitor, and k' is the binding constant. Fig. 6 indicates linear relationship between log Θ / 1- Θ and log C at different temperatures, and the calculated values of 1/y and K are given in Tables 6 and 7.

The free energy of adsorption (ΔG_{ads}) at different concentrations of the natural products as calculated from the following equation:

$$\Delta G_{ads} = -RTLn(55.5 K) \tag{11}$$

Where the value 55.5 is the molar concentration of water in the solution mol/1.

The values of ΔG_{ads} are given in Table 7 and negative values in all cases means that spontaneous adsorption of inhibitor on steel surface and strong interaction between the inhibitor molecules and metal surface. The (ΔG_{ads}) values are negative and lie in the range of (32–38) $kJmol^{-1}$ for Flory - Huggins and (15–17) KJ mol^{-1} for kinetic isotherm. It's found that (ΔG_{ads}) values are more positive than -40 $Kjmol^{-1}$ indicating that the inhibitors are physically adsorbed on the metal surface. The results have also been reported by J. D. Talati. [39]
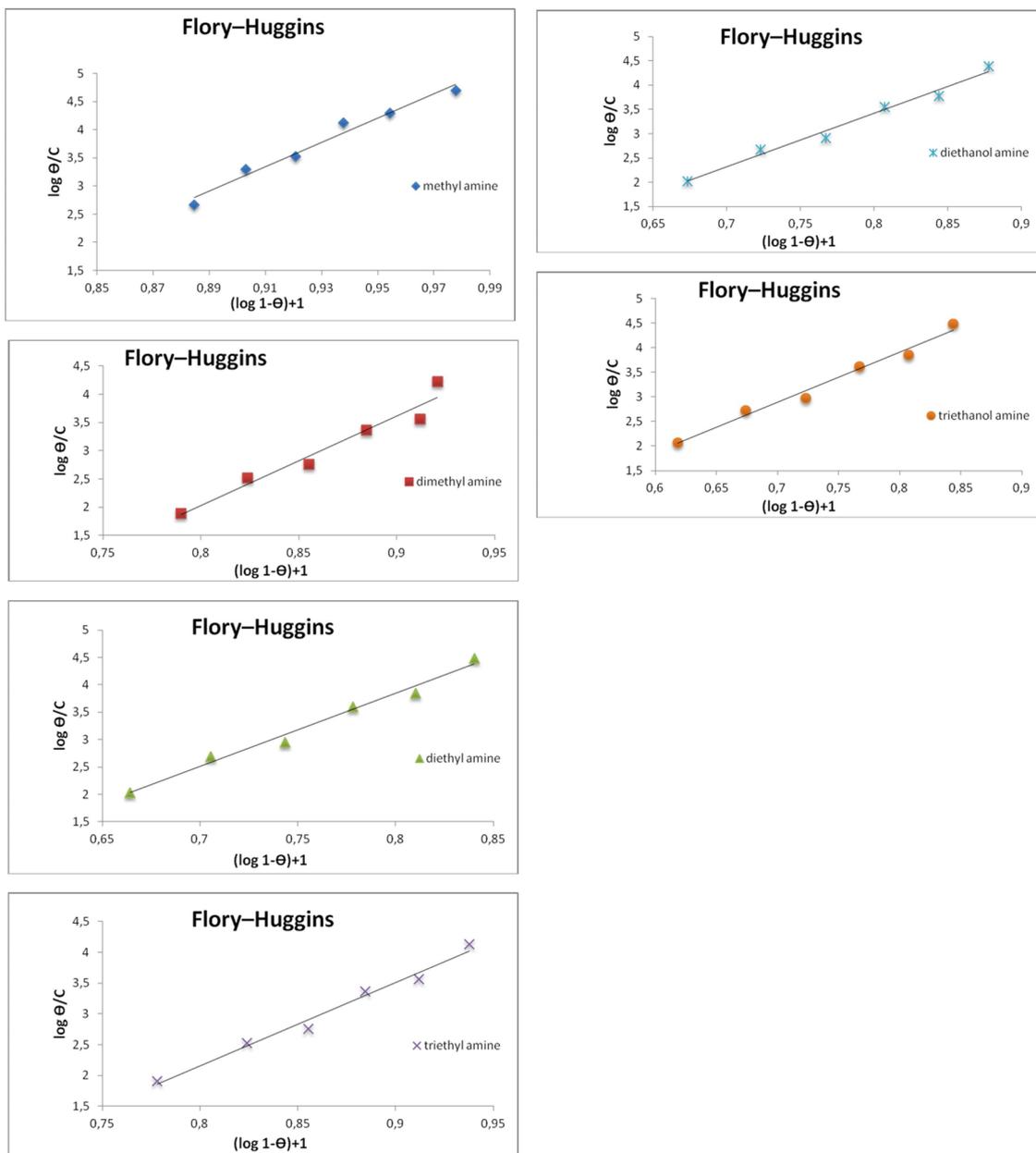
Fig. 5. Flory–Huggins adsorption isotherm at 298 k for different amines.

3.4. Effect of temperature

The temperature effect on the Fe anodic corrosion rate in absence and presence of amines was determined in the temperature range between (25 °C–40 °C). It was observed that the anodic corrosion rate increased with raise in temperature for the different concentrations of amine. The values of E_a that have been calculated from the slopes of Arrhenius plots [40,41]

$$\log I = Log\ A - E_a\ /\ 2.303\ R\ T \tag{12}$$

where I is the limiting current, A is apre-exponential factor, R is the universal gas constant and T is the absolute temperature.

Figures (7, 8, 9,10, 11,12) represent the relation between ln I and 1/T for blank solution and for different concentrations of Amines (methyl amine, dimethyl amine, diethyl amine, triethyl amine, diethyl amine, triethanol amine respectively), this Figure shows straight lines and the value of E_a have been derived from slopes of Arrhenius plots and are giving in Table 8. It is obviously seen that E_a values in absence and presence of the Hibiscus extract are less than 40 k.J.mol^{-1} indicating that the anodic corrosion reaction is under a diffusion control [42].

3.4.1. Thermodynamic treatment of the results

From the integrated form of Arrhenius equation:

$$\ln I = -E_a\ /\ RT + \ln A \tag{13}$$

Fig. 6. The Kinetic Thermodynamic isotherm at 298 k for different amines.

Fig. 7. The relation between the natural logarithm of the limiting current and $1/T$ for methyl amine at different concentrations ($\mathbf{mol.l^{-1}}$).

$$\Delta G^* = \Delta H^* - T \Delta S^* \tag{16}$$

where k is Boltzmann 's constant, e = 2.7183, h is Plank 's constant, T is absolute temperature and R is the universal gas constant. Adsorption is usually followed by liberation of heat of adsorption, so that $E_a < 0$, consequently, the rate of adsorption decreases with raise in temperature and as a result, the surface coverage, Θ, at given concentration decreases with increasing temperature. It is known that an increase in the heat of adsorption leads to an increase in the energy of adsorption. However rising of temperature acts in the reverse direction, increasing the kinetic energy of molecules, facilitating disruption (consequently in the physical adsorption).

Table 8 shows that the entropy ΔS^* posses high negative values are indicating highly ordered natural products in the solution under investigation. These values found to be independent on the type of natural Products.

Variation in the rate within a reaction series may be caused by changes in either, or both, the enthalpy or the entropy. The correlation between ΔH^* and ΔS^* is a linear relationship may which could be stated algebraically as (Fig. 8)

$$\Delta H^* = \beta \Delta S^* + \text{constant} \tag{17}$$

$$\delta \Delta H^* = \beta \Delta S^* \tag{18}$$

The operator, δ, concerns difference between any two reactions in series. Substituting from the Eq. (11) into the familiar relationship:

$$\delta \Delta H^* = \delta \Delta G^* + T \delta \Delta S^* \tag{19}$$

We obtain

$$\beta \delta \Delta S^* = \delta \Delta G^* + T \delta \Delta S^* \tag{20}$$

It follows that when $\delta \Delta G^* = $ zero, then $\beta = T$. In other words, the slope in a linear plot of δH^* versus ΔS^* is the temperature at which all reactions that conform to the line occur at the same rate. β is therefore known as the isokinetic temperature. The isokinetic plot of ΔH^* and ΔS^* for different concentrations of the natural products under study. Fig. 9 and Table 8 was found to be linear and the isokinetic temperature (β) was computed from the slope of the plot as 353 K using divided cell. These values are much higher than that of the experimental temperature 298 K, indicating that the rate of the reaction is enthalpy controlled (40), (41).

where: I is the rate cefficient (rate constant), R is the gas constant (8.314 kJ. mol^{-1}), E_a is the activation energy (kJ.mol^{-1}) and A is the frequency factor. It can be seen that the gradient is given by $-E_a/R$ and intercept by lnA. Table 8 gives the values of E_a for the natural products used. The values of enthalpy ΔH^*, entropy ΔS^*, and free energy (ΔG^*) can be obtained by the equations:

$$\Delta H^* = E_a - RT \tag{14}$$

$$\Delta S^* / R = \ln (k T_e / h) \tag{15}$$

Table 8

thermodynamic parameters for (a) methyl amine, (b) dimethyl amine, (c) diethyl amine, (d) triethyl amine, (e) diethanol amine and (f) triethanol amine.

Compound (a)

Conc.*10^5 mol.l^{-1}	E_a^* (kJ.mol^{-1})	ΔH^* (kJ.mol^{-1})	Δ- S * (kJ.mol^{-1})	ΔG^* (kJ.mol^{-1})
0	8108	6885	−168.5	57109
1	1236	5174	−183.3	58405
5	5224	3699	180.2	58506
10	5698	3131	−182.4	57512
50	6757	3320	−182.1	58724
100	7504	3550	−181.66	58820
500	6624	3799	−181.24	58943

Compound(b)

Conc.*10^5 mol.l^{-1}	E_a^* (kJ.mol^{-1})	ΔH^* (kJ.mol^{-1})	Δ- S * (kJ.mol^{-1})	ΔG^* (kJ.mol^{-1})
0	9427	6888.23	−168.56	58797
1	10548	8306	−165.28	59215
5	9504	6965	−170.05	59341
10	10067	7528	−168.69	59485
50	10701	8162	−167.12	59636
100	11420	8882	−165.3	59797
500	11255	8717	−166.47	59992

Compound (c)

Conc.*10^5 mol.l^{-1}	E_a^* (kJ.mol^{-1})	ΔH^* (kJ.mol^{-1})	Δ- S * (kJ.mol^{-1})	ΔG^* (kJ.mol^{-1})
0	12082	9543	−159	58530
1	14870	12332	−152.7	59365
5	15784	13245	−150.2	59509
10	16820	14208	−147.3	59662
50	18001	15463	−144	59826
100	19364	16825	−140	60001
500	21963	19424	−132.2	60166

Compound (d)

Conc.*10^5 mol.l^{-1}	E_a^* (kJ.mol^{-1})	ΔH^* (kJ.mol^{-1})	Δ- S * (kJ.mol^{-1})	ΔG^* (kJ.mol^{-1})
0	9427	6888	−168.5	58797
1	9004	6465	−171.2	59184
5	9507	6968	−170	59318
10	10069	7530	−168.6	59459
50	10702	8163	−167	59609
100	11764	9662	−164	59780
500	13531	10992	−159.9	59945

Compound (e)

Conc.*10^5 mol.l^{-1}	E_a^* (kJ.mol^{-1})	ΔH^* (kJ.mol^{-1})	Δ- S * (kJ.mol^{-1})	ΔG^* (kJ.mol^{-1})
0	8141	5819	−174	59428
1	10491	7952	−168.4	59818
5	11255	8717	−166.5	5992
10	12140	9601	−164.2	60178
50	13176	10637	−161.5	60378
100	14871	12332	−165.6	60574
500	15893	13354	−154.1	60834

Compound (f)

Conc.*10^5 mol.l^{-1}	E_a^* (kJ.mol^{-1})	ΔH^* (kJ.mol^{-1})	Δ- S * (kJ.mol^{-1})	ΔG^* (kJ.mol^{-1})
0	8108	5819	−174.1	59428
1	1236	1301	−195.3	61468
5	5224	2686	−187.2	60332.8
10	5698	3159	−186.3	60546
50	6757	4218	−183.7	60795
100	7504	4965	−182.1	61053
500	6624	4085	−186.14	61428
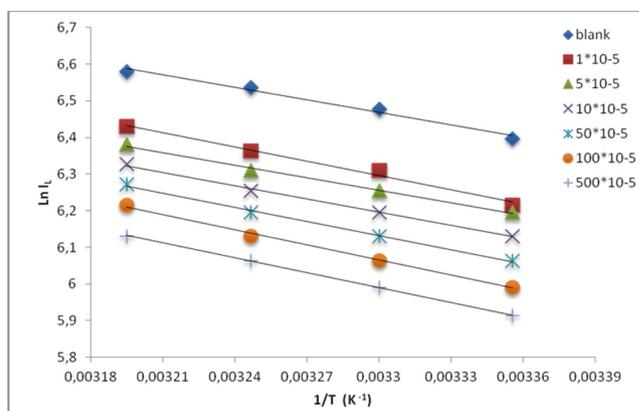
Fig. 8. The relation between the natural logarithm of the limiting current and 1/T for dimethyl amine at different concentrations (**mol.l^{-1}**).
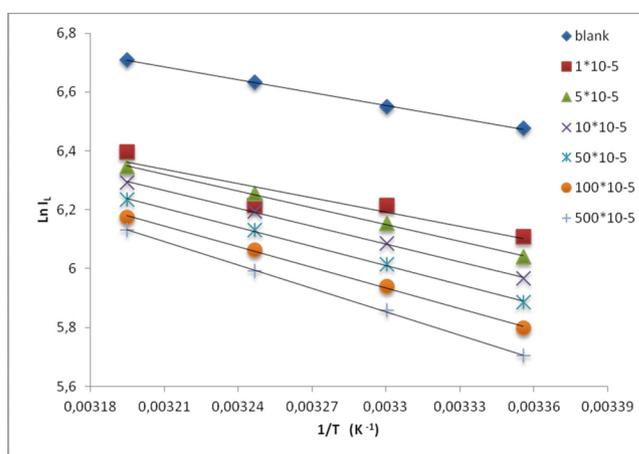
Fig. 9. The relation between the natural logarithm of the limiting current and 1/T for diethyl amine at different concentrations (**mol.l^{-1}**).
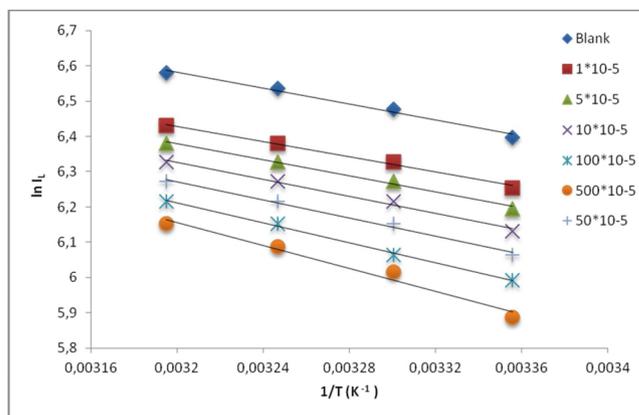
Fig. 10. The relation between the natural logarithm of the limiting current and 1/T for triethyl amine at different concentrations (**mol.l^{-1}**).

3.5. Structure effect of organic additives

Many additives are known to be capable of adsorption on the anodic substrate, it also can trap in the corrosion over potential. This is due to either the need for electron transfer to occur through the adsorption layer or to form a complex at the electrode surface. A complication of
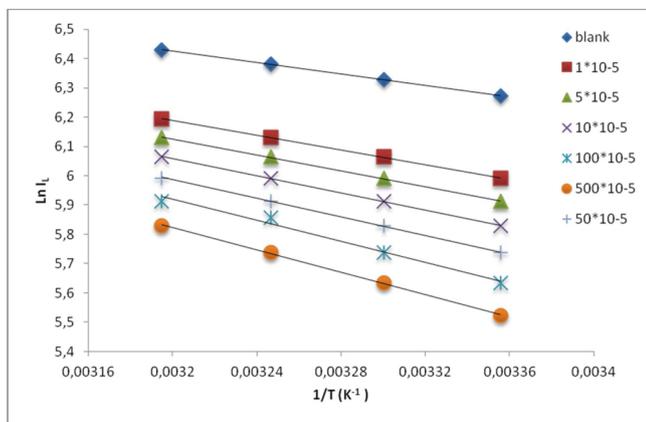
Fig. 11. The relation between the natural logarithm of the limiting current and $1/T$ for diethanol amine at different concentrations (.**mol.l^{-1}**).
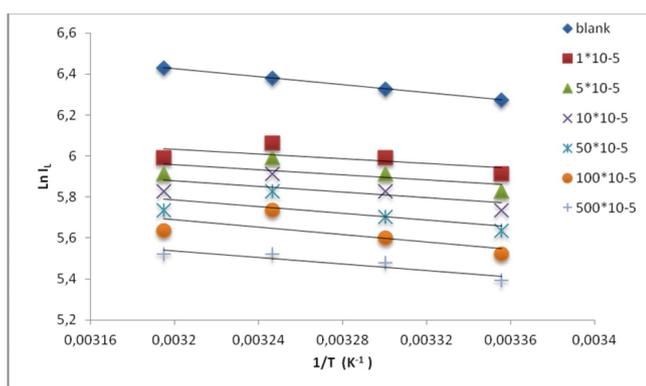
Fig. 12. The relation between the natural logarithm of the limiting current and $1/T$ for Triethanol amine at different concentrations (**mol.l^{-1}**).
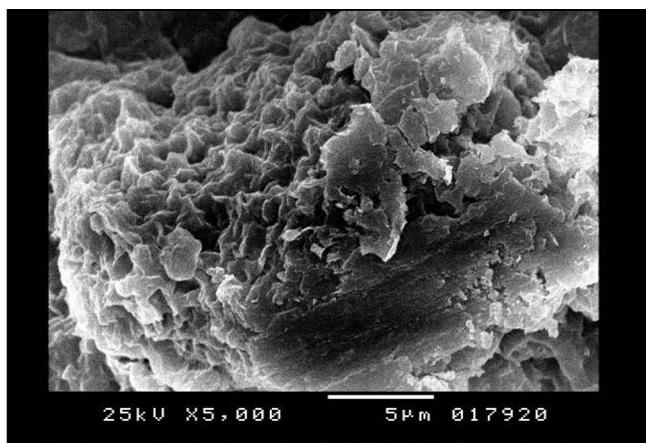
Blank

Fig. 13. STM (Scanning Electronic Microscopy) of polished steel metal in absence of organic amine compounds.

the metal cation in the solution is also proposed. In many cases, the use of additives is still done in empirical way. Indeed, there are very large numbers of both organic and non-organic substance that can be used. Moreover, their action could be different in function of the substrate,

the ion to reduce and the electrolytic condition. For example, re-orientation of the additives on the electrode surface has been observed depending on the surface coverage or pH.

In case of steel, and because of its industrial interest a numbers of researcher have already been undertaken. A complex in solution between amines derivatives and Fe^{2+} cation is formed as a result of transport of steel ions from the interface to the bulk and the work for the discharge of steel complex ion increase.

The study of the effect of nitrogen free amines compounds, on the corrosion process is illustrated by adsorption curves. The efficiency of inhibition decreases in the order: triethanol amine > diethanol amine > triethyl amine > diethyl amine > dimethyl amine > methyl amine.

In acidic medium, N- atom tends to be protonated from acid at the anode steel surface. The above behavior may also be able to discuss on the basis that, triethanol amine and diethanol amine are more inhibitors because the ethanol group is nucleophilic group would lead to more convenient electron density on N-atom. This might led to more convenient electron transfer from functional group to metal anode with subsequent coordination, leading to greater adsorption and inhibition efficiency (Figs. 10–12).

3.6. Scanning electronic microscopy measurements (SEM)

Effect of adding organic additives on the scanning electronic microscopy has been studied. All experiments were carried out at the limiting current determined at 293 K and time of 5 min. Fig. 13 shows the morphology of polished steel metal in absence of organic amine compounds as blank, It can be noticed that under the corrosion layer the initial structure of the unexposed materials can be observed and some holes constituted by accumulation of several cabbage. While, Figs. 14–19 show the morphology of polished steel metal in presence of different organic amine compounds in 8 M H_2SO_4 at the limiting current determined at 293 K and time of 5 min in different concentrations of amine compounds (1×10^{-5}, 50×10^{-5} mole l^{-1}). These figures show that the presence of some holes constituted of several cabbage, the number of holes decreases in the order of triethanol amine > diethanol amine > diethyl amine > Triethyl amine > dimethyl amine > methyl amine. On the other hand a highly surface roughness appear and some cracks appear which decrease by increasing concentrations from 1×10-5 mol/l to 50×10-5 mol/l

4. Conclusions

The following conclusions arise from the work described here in:

1 A typical polarogram is obtained in this study for triethanol amine in case of divided and undivided cell. The curve is divided into three parts: in the first part, the current density (c.d) is proportional to the voltage. At the second part of the curve, the metal undergoes electro-polishing. In the first part, etching takes place and in the last part, some localized pitting occurs

2 The observed limiting current, which represents the rate of Steel metal anodic corrosion in phosphoric acid at different temperature, are found that, the limiting current decrease with increasing the concentration of organic amines.

3 The inhibition percent that caused by organic amines range from 5% to 59.9% depending on amine type and its concentration.

4 The inhibition efficiency of homologous series of organic substances, differ only in the heteroatom, is usually in the following sequence: **P > Se > S > N > O**

5 The values of ΔG_{ads} are given in negative values in all cases means
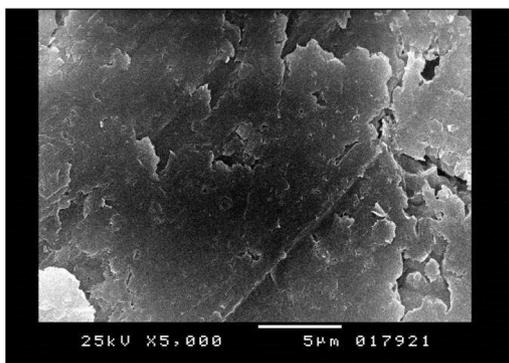
Cpd I 1 (1x10^{-5} mole l^{-1}).   Cpd I 2(50x10^{-5} mole l^{-1}).

Fig. 14. STM (Scanning Electronic Microscopy) of polished steel metal in presence of methyl amine compounds.
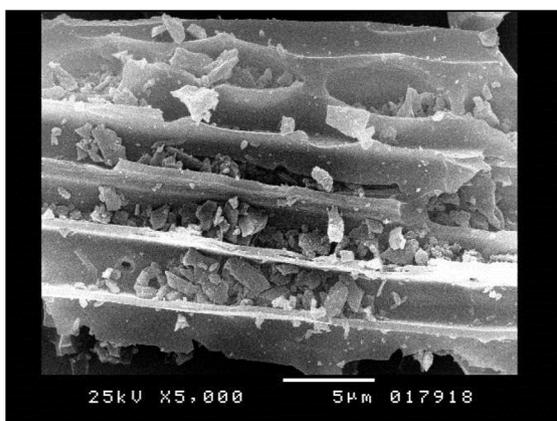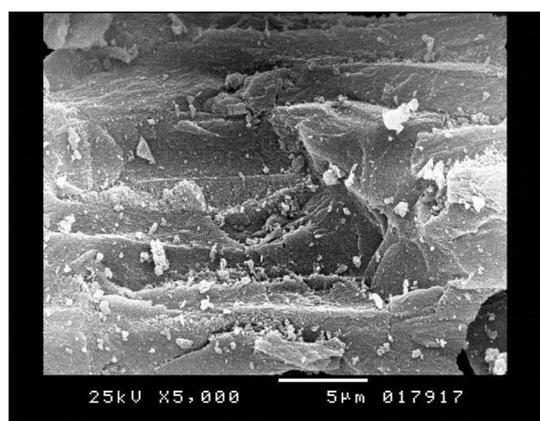
Cpd II 1   (1x10^{-5} mole l^{-1}).   **Cpd II 2**(50x10^{-5} mole l^{-1}).

Fig. 15. STM of polished steel metal in presence of dimethyl amine compounds.
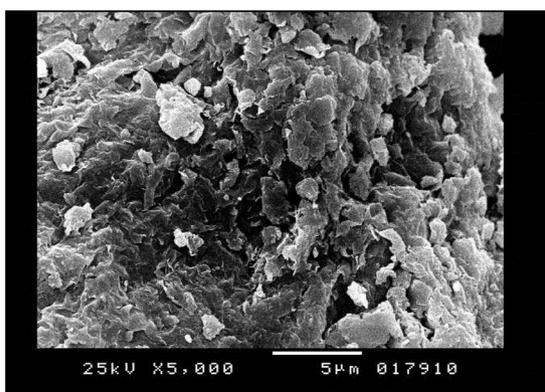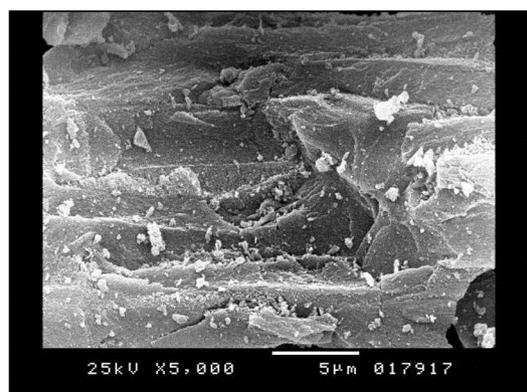
Cpd III 1   (1x10^{-5} mole l^{-1}).   **Cpd III 2**(50x10^{-5} mole l^{-1}).

Fig. 16. STM of polished steel metal in presence of diethyl amine compounds.

Cpd IV 1(1×10^{-5} mole l^{-1}).
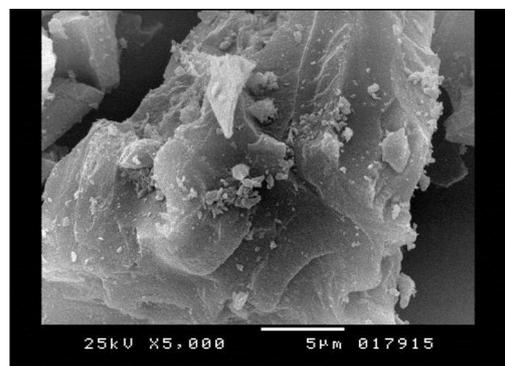
Cpd IV 2(50×10^{-5} mole l^{-1}).

Fig. 17. STM of polished steel metal in presence of Triethyl amine compounds.

Cpd V 1   (1×10^{-5} mole l^{-1}).
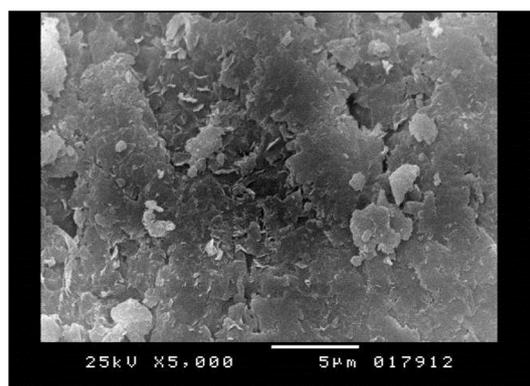
Cpd V 2(50×10^{-5} mole l^{-1}).

Fig. 18. STM of polished steel metal in presence of diethanol amine compounds.
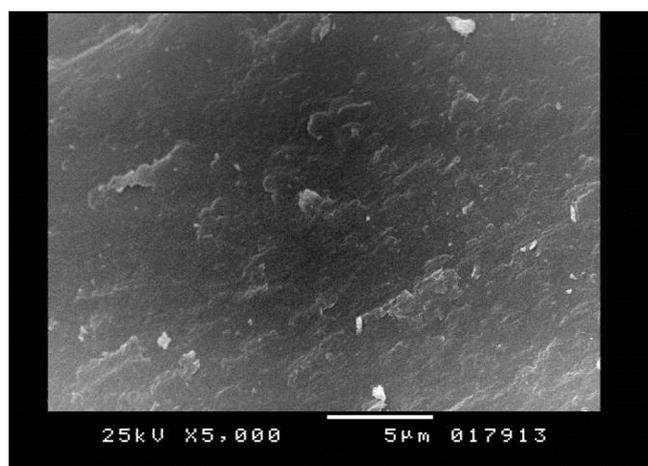
Cpd VI (50×10^{-5} mole l^{-1}).

Fig. 19. STM of polished steel metal in presence of Triethanol amine compounds.

that spontaneous adsorption of inhibitor on steel surface and strong interaction between the inhibitor molecules and metal surface. It lies in the range of (32–38) kJmol^{-1} for Flory - Huggins and (15–17) KJ mol^{-1} for kinetic isotherm. It's found that (ΔG_{ads}) values are more positive than -40 Kjmol^{-1} indicating that the inhibitors are

physically adsorbed on the metal surface.

6 It was observed that the anodic corrosion rate increased with raise in temperature for the different concentrations of amine.

7 It is obviously seen that E_a values in absence and presence of the Hibiscus extract are less than 40 k.J.mol^{-1} indicating that the anodic corrosion reaction is under a diffusion control

8 The efficiency in inhibition decreases in the order: triethanol amine > diethanol amine > triethyl amine > diethyl amine > dimethyl amine > methyl amine.

References

[1] W.J. NcTegart, The Electrolytic and Chemical Polishing of Metals, Pergamon Press, London, 1956.
[2] J.F. Jumer, Metal Finishing Guidebook and Directory, Metals and Plastics Publications, Hackensack, New Jersey, 1972.
[3] P.V. Shigolev, Electrolytic and chemical polishing of metals, Freund Tel-Aviv (1974).
[4] W. Schwartz, Plat. Surf. Finish. 68 (1981) 42.
[5] W.C. Elmore, J. Appl. Phys. 10 (724) (1939).
[6] J. Edwards, J. Electrochem. Soc. 100 (1953) 223.
[7] M.C. Petit, Electrochim. Acta 8 (1963) 217.
[8] T.P. Hoar, G.P. Rothwell, Electrochim. Acta 9 (1964) 135.
[9] S.I. Krichmar, Russ. J. Phys. Chem. (Engl. Transl.) 39 (1965) 433.
[10] K. Kojima, C.W. Tobias, J. Electrochem. Soc. 120 (1973) 1026.
[11] R. Kircheim, K. Maier, G. Tolg, J. Electrochem. Soc. 128 (1981) 1027.
[12] S.H. Glarum, J.H. Marshall, J. Electrochem. Soc. 132 (1985) 2872.
[13] M. Turner, G.E. Tompson, P.A. Brook, Corros. Sci. 13 (1973) 985.
[14] l. Alains, D.J. Shriffrin, Electrochim. Acta 27 (1982) 837.
[15] L. Ponto, D. Landolt, J. Appl. Electrochem. 17 (1987) 205.
[16] D.R. Gabe, Corros. Sci. 13 (1973) 175.
[17] L. Ponto, M. Datta, D. Landolt, Surf. Coat. Technol. 30 (1987) 265.
[18] R. Lalitha, S. Ramesh, S. Rajeswari, Electrochim. Acta 51 (2005) 47.

[19] X. Li, S. Deng, Corros. Sci. 53 (2000) 664.
[20] M. Eiesenberg, C.W. Tobias, C.R. WilKe, J. Electrochem. Soc. 101 (1999) 306–320.
[21] M.G. Fouad, F.Z. Zein, M.I. Ismail, Electrochem. Acta 9 (1972) 150.
[22] G.M. El-Subruiti, A.L. Kawana, J. Appl. Sci. 10 (1995) 318.
[23] L.H. Jenkins, R.B. Durham, J. Electrochem. Soc. 11 (1976) 768.
[24] J.D. Talati, J.M. Pandya, Br. Corros. J. 16 (1976) 603.
[25] A.A. ATaha, Bull. Electrochem. 9 (2&3) (1993) 80.
[26] A.M. Ahmed, G.B. Mohamed, J. Chin. Chem. Soc. (Taiwan) 42 (1989) 78.
[27] F. Donnue, K. Nobe, J. Electrochem. Soc. 112 (1965) 886.
[28] G.J. Poling, Electrochem. Soc. 114 (1967) 1209.
[29] T. Murhawa, S. Kato, N. Nagura, Ilackerman, Corros. Sci. 8 (1958) 341.
[30] Y. Mat' Ioa, Y. Kinuhata, M. Okahara, S. Komari, H. Tamura, Corrosion 10 (1973) 557.
[31] M. Kaminiski, and Szhlarska-Simiallowska, Z Corros. Sci. 13 (1973) 557.
[32] Atega, Br. J. Electroanal. Chem. 76 (1977) 191.
[33] K. Nobc, N. Eidakar, Corrosion 37 (1951) 271.
[34] N. Hackerman, R. Hard, Butterworths, LondonProceedings of Ist International Congress on Metallic Corrosion1962, Proceedings of Ist International Congress on Metallic Corrosion (1962).
[35] B. AI-Anadouli, F. Eltaib, F. El-Nizami, Extended Abstracts Of The Electrochemical Soc. Fall Meeting, Chigco, (1988), p. 188.
[36] R.M. Hurd, N. Hackerman, Proceedings of 1st International Congress on Metallic Corrosion, Butterworths, London, 1962, p. 166.
[37] A.N. Frumkin, Z. Phys, Eng. Chem. 116 (1925) 446–462.
[38] E.E. Ebenso, U.J. Ekpe, B.I. Ita, O.E. Offioing, Mater. Chem. Phys. 60 (1999) 79–90.
[39] J.D. Talati, J.M. Darji, J. Ind. Chem. Soc. 65 (1988) 94–99.
[40] E.N. Noor, Mater. Chem. Phys. 114 (2009) 533–540.
[41] M. Eiesenberg, C.W. Tobias, C.R. WilKe, J. Electrochem. Soc. 101 (1990) 306–320.
[42] A.M. Mousaa, M.M. El-Banna, I.A.S. Mansour, Bull. Electrochem. 7 (1991) 164–174.